Spectroscopy of growth islands in GaAs/$In_{0.1}Ga_{0.9}As$/AlAs double-barrier structures from photoluminescence and resonant tunneling studies

Y. Galvão Gobato*
Departamento de Física, Universidade Federal de São Carlos, CP 676, São Carlos-SP, 13565-905, Brazil

A. L. C. Triques,† P. H. Rivera,‡ and P. A. Schulz
Departamento de Física do Estado Sólido e Ciéncias dos Materiais, Instituto de Física Gleb Wataghin, CP 6165, Campinas-SP, 13083-970, Brazil

(Received 30 October 1998)

Photoluminescence spectroscopy is used to investigate interface roughness effects on electron and hole tunneling through GaAs/$In_{0.1}Ga_{0.9}As$/AlAs double-barrier tunneling structures. Typical quantum-well photoluminescence spectra present a splitting of 8 meV due to interface roughness and island formation in the quantum well. The states of these islands are selectively populated by electrons and holes by applying bias and changing the photon excitation intensity. Carrier transfer mechanisms between islands are clearly identified as well as intersubband scattering in a sequential tunneling picture. The measurement of activation energies as a function of bias provides an estimate for the electron density in resonant tunneling condition for diodes showing up islands at the interfaces. The possibility of observing growth island effects in $I(V)$ characteristics is also carefully discussed. [S0163-1829(99)06231-1]

I. INTRODUCTION

The resonant tunneling effect has proved to be an important tool for the spectroscopy of new physical phenomena. Here one could mention the observation of quantum chaos effects,[1] Fermi edge singularity,[2] quantum dot states,[3] and effects of intense ac electric fields on electronic states in quantum wells and superlattices.[4] Photoluminescence (PL) and photoluminescence excitation (PLE) spectroscopies have been used to provide important insight into tunneling dynamics, like the charge buildup in the double-barrier quantum well under resonant tunneling conditions.[5–8] Recently, PL studies have also shown the formation of electron-dressed excitons (X^-) in quantum wells of tunneling structures.[9–11] On the other hand, PL and PLE are useful techniques to investigate interface roughness effects in semiconductor heterostructures.[12,13] The effects of roughness upon tunneling[14] are expected to be important when the deviation in thickness is a sizable fraction of a tunneling barrier, electron wavelength, or quantum-well width.[15,16] Such effects have been measured in PL and PLE spectra in quantum wells with thin barriers[17,18] and in electron transport.[19] Nevertheless, the precise nature of interface roughness in semiconductor heterostructures is a complex task and is sensitive to many epitaxial growth parameters such as temperature, growth times, substrate orientation, or growth constituent flux ratio.[12,13]

In the present paper, we study interface roughness effects on GaAs/$In_{0.1}Ga_{0.9}As$/AlAs tunneling structures in a triple-well configuration.[20] We investigate electron transport and PL spectra under applied bias for different photoexcitation intensities on a wide temperature range. We observe a splitting in the quantum-well PL and PLE spectra under resonant tunneling condition, which are related to growth island formation. The states of these islands are selectively populated by electrons and holes by applying bias and changing the photoexcitation intensity. Carrier transfer mechanisms between islands are clearly identified as well as intersubband scattering in a sequential tunneling picture. The measurement of activation energies as a function of bias provides an estimate for the electron density in resonant tunneling condition for diodes showing up islands at the interfaces. On the other hand, study of growth island effects[16] in tunneling spectroscopy is revealed to be an involved task due to the fact that these effects would lead to signatures in the I-V characteristics that are similar to features related to the tunneling charge redistribution in the emitter[21] and transport measurements alone may not be enough to differentiate both contributions.

The present work can be included in a broader context, namely, the optical properties related to spatially separated regions of a given two dimensional system. Other recently studied similar examples are extremely thin quantum wells showing up a morphology of islands connected by wetting layers,[22] as well as corrugated quantum wells developing structures of quantum-well wires alternated with quantum-well regions.[23]

II. EXPERIMENTAL DETAILS

Our sample was grown by molecular beam epitaxy on a GaAs [100] semi-insulating substrate and consists of two 50 Å AlAs layers (barriers) and three 50 Å $In_{0.1}Ga_{0.9}As$ layers (quantum well). This intrinsic region was sandwiched between two 50 Å GaAs spacer layers and 100 Å of GaAs $n^+(1\times10^{17}\,cm^{-3})$, followed by 5000 Å of GaAs $n^+(3\times10^{18}\,cm^{-3})$ on each side, one on the top, the other on the bottom of the structure. We have intentionally limited the indium content of $In_xGa_{1-x}As$ layers to 0.1 in order to avoid misfit dislocations.[20] A 5 Å thick GaAs spacer was placed between AlAs and $In_xGa_{1-x}As$ layers to recover good sur-

face quality.[17] Standard mesa etching techniques were used to define square mesa devices of $186\times116\,\mu m^2$ with a 980 μm^2 aperture in the top contact for optical access.

We have measured current-voltage $I(V)$ characteristics, and photoluminescence and photoluminescence excitation spectra under bias voltage at several temperatures and photoexcitation intensities. The voltage is measured with the use of a pseudo-four-terminal technique. The optical measurements were performed using an argon-ion pumped tunable Ti:sapphire laser as excitation source. The luminescence signal was dispersed in a 0.75 m double-grating spectrometer and detected by a thermoelectrically cooled GaAs photomultiplier. Two excitation conditions were used: (i) photon energy equal to 1.55 eV, near the energy gap of the contacts; (ii) photon energy equal to or greater than 1.68 eV, which is above the $In_{0.1}Ga_{0.9}As$ midwell fundamental optical transition energy.

In the first case (i), the photoexcitation takes place only in the contact region and the photoluminescence signal arises from the contact layers at zero bias. For suitable applied voltages, resonant tunneling occurs and electrons and holes can also recombine in the midwell, giving rise to the quantum-well luminescence. In the second case, (ii), carriers are excited not only in the contact region but also in the quantum-well layers. Therefore, if the sample is biased, the midwell luminescence arises from tunneling electrons and holes and also those photoexcited in the well region. For the sake of simplicity, without losing generality, most of the work will be concentrated on case (i) situations.

III. RESULTS AND DISCUSSION

A. Low excitation intensity

The experimental situation for tunneling properties is summarized in Fig. 1. The conduction and valence potential profiles of the structure, obtained by a Poisson solver which combines a semiclassical approximation for the electrons in the contacts with a more appropriate treatment of two dimensional (2D) electrons in the emitter,[21] are shown in Fig. 1(a). The $In_{0.1}Ga_{0.9}As$ layer adjacent to the emitter barrier forms a prewell, where electrons can accumulate into 2D states isolated from the emitter contact by a potential bump in the spacer layer region. The midwell controls the escape process whereas the postwell preserves the symmetry of structure. The resonant tunneling process is determined by the competition between two tunneling channels: (i) 3D electrons of the far emitter contact, launched over the spacer layer hump, tunneling directly through the midwell; and (ii) coupling of quantized levels in the prewell and midwell. For high barriers, as in the present case, channel (i) would show up as a small bump at the onset of resonant tunneling in a $I(V)$ curve, while channel (ii) would be related to the peak current.[21] The experimental current-voltage characteristics obtained for this sample at 2 K are shown in Fig. 1(b), showing a slight asymmetry: at forward bias the resonance is observed at 0.35 V and for reverse bias at 0.38 V. A possible distinction between two tunneling channels, regarding the dimensionality of the electrons in the emitter contact, discussed above, can be the origin of the feature observed in the derivative of the $I(V)$ curve near the onset of resonant tunneling, Fig. 1(c).

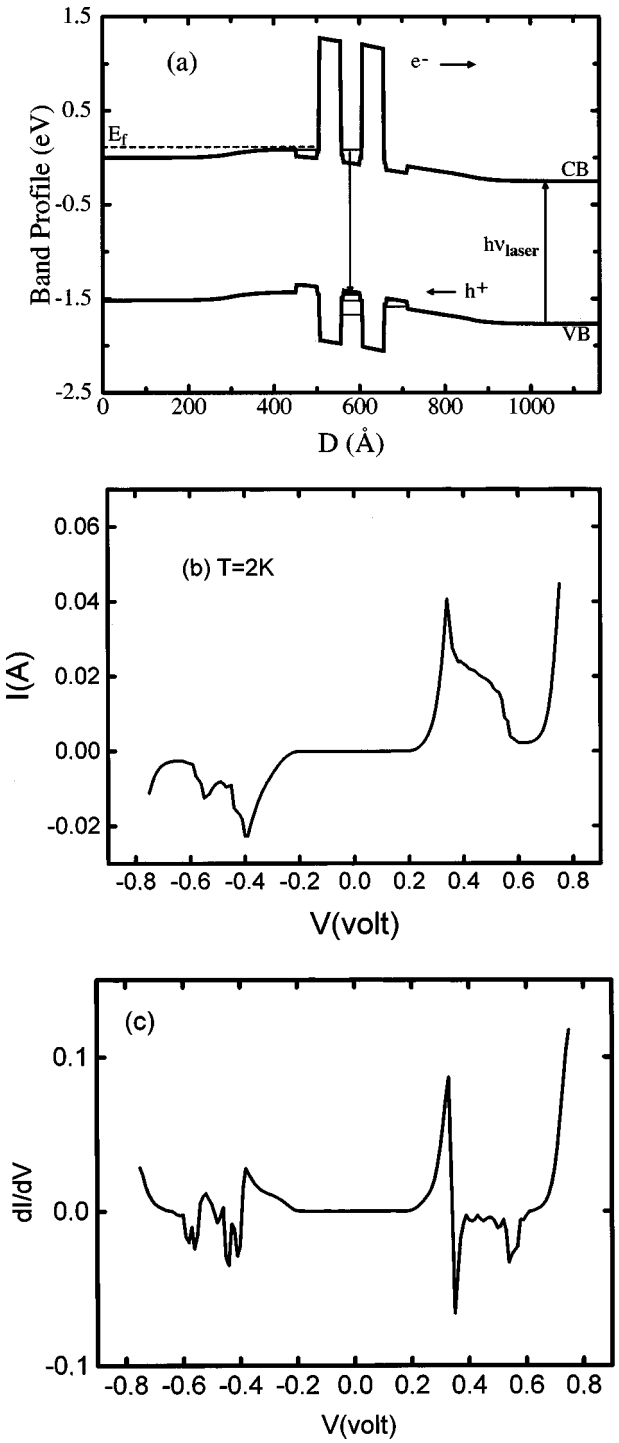

FIG. 1. (a) Calculated conduction and valence band profiles at the resonance voltage. The dashed line indicates the Fermi level in the emitter. (b) Experimental current-voltage characteristics of the device measured at 2 K. (c) First derivative of the $I(V)$ characteristic shown in (b).

Since in the following we will be concerned with optical measurements under applied bias, it should be mentioned for the sake of clarity that forward (reverse) bias means top negative (positive) biased contact. One should keep in mind, however, that the results shown here are qualitatively independent with respect to bias polarization, since electron-hole pairs will be excited on both contact regions in the actual experimental setup. The very important parameter will be the

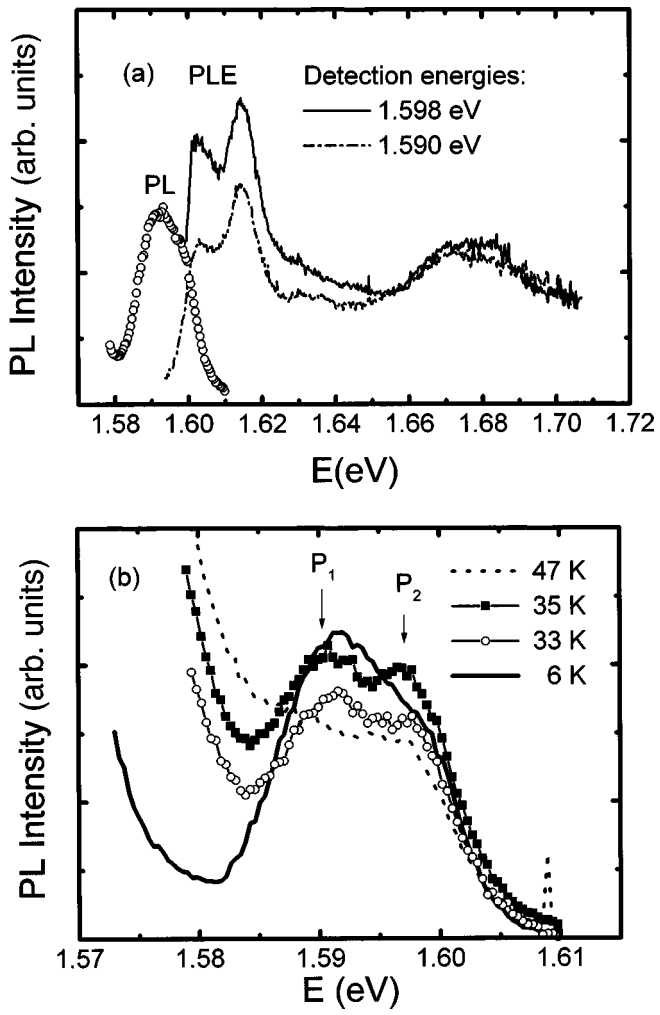

FIG. 2. (a) PL and PLE spectra for the structure at zero bias for $T=2$ K. (b) Temperature dependence of PL spectra at zero bias for excitation energy of 1.68 eV. P_1 and P_2 are the two luminescences related to the double peak in the PLE shown in (a) (see text).

electron injection in the quantum well by applying bias. In this work we show results for reverse bias polarization. Besides, having this picture in mind, a small quantum-well PL signal may also be expected even in the absence of bias for high energy photon excitation directly in the midwell.

Figure 2 shows the quantum-well PL and PLE spectra at zero bias ($V=0$). Besides the very strong and broad PL from the GaAs contact layers at 1.51 eV, an extra PL line near 1.59 eV is observed, related to the E_1-HH_1 transition in the midwell. We have identified the observed peaks by calculating the transition energies as a function of well width in a single $In_{0.1}Ga_{0.9}As/AlAs$ quantum well taking into account the stress induced by lattice mismatch between the $In_{0.1}Ga_{0.9}As$ and the AlAs layer. The first remarkable feature of these results is that both PL and PLE profiles reveal a double-peak structure for this fundamental transition, Fig. 2(a). According to our calculation, a well width variation of one monolayer can be the origin for this amount of energy splitting, suggesting island formation in the structure. Indeed, the following results will support this interpretation. Each PL line is associated to recombinations at islands characterized by a given width in the mid quantum well. This width fluctuates, in the present case, by one monolayer on average, defining regions (islands) of two different widths. Typically, the splitting occurs when the size of the growth island exceeds the diameter of the exciton. This splitting of 8 meV is clearly observed in the PL spectra at higher temperatures ($T\sim 30$ K) [Fig. 2(b)] and will be discussed in detail later. In the following, we will label the lowest energy line P_1 and the highest energy line P_2. The number of peaks is related to the set of monolayer fluctuations at the interfaces. A variety of results has been reported, showing up to four or even eight monolayer fluctuations.[12,13] A set of only two island thicknesses is a quite common situation and has been reported previously.[24,25] In particular, Tsuchiya, Matsutue, and Sakaki[25] measured tunneling escape times for unbiased quantum wells, but could not resolve effects due to monolayer fluctuations in the well width on these times.

The PLE spectra at zero bias, detected at both quantum-well (QW) lines, present an excitonic peak associated to the fundamental excitonic absorption, E_1-HH_1. This peak presents a splitting of 11 meV, which evidences a transfer of excitons between different islands in the QW. A second exciton peak is also observed at nearly 1.67 eV and corresponds to the E_1-HH_2 transition in the midwell. The large Stokes shift observed in Fig. 2, $S=12$ meV, is an evidence of strong microroughness combined with alloy disorder, superposed to the islands, at the interfaces. Such a large Stokes shift is comparable to the PL linewidths, as observed in many other quantum-well systems. Nevertheless, our results show some peculiarities which deserve a further comment. The linewidths $W\approx 8$ meV refer to single peaks obtained by the PL spectra fitting, as described below in reference to Fig. 4. The ratio $\gamma=S/W\approx 1.5$ is larger than for other results,[26] which follow a rather universal behavior of $\gamma\approx 0.6$, well described by an interface fluctuation model proposed by Wilkinson *et al.*[26] This model does not take into account alloy disorder. Nevertheless, a rough estimation shows that $\gamma\approx 1.9$ for bulk alloys.[26] Other recent numerical simulations of excitonic behavior in quantum wells take into account alloy disorder together with short range potential fluctuations at the interfaces,[27] but disregarding island structures. The present work deals with the interesting situation where the monolayer confinement energy difference is of the same order as the linewidths as well as the Stokes shift. The relatively high γ ratio suggests the importance of alloy disorder in order to meet this situation.

At this point it should be noticed that it is difficult to get this information solely from the I-V characteristics, which in the present case exhibits a relatively high peak-to-valley ratio. One would expect that the double-peak structure in the PL, due to growth islands, could be resolved in the tunneling current measurement, as recently predicted by Dietze and Darling[15] and Wang *et al.*[16] The presence of a strong microroughness, broadening the resonances, leads to a situation in which the islands are still resolved in PL measurements, but not in a less sensitive spectroscopy like the I-V characteristics.[28] One could speculate if the feature in the derivative of the $I(V)$ characteristic shown in Fig. 1(c) could be related to the widest islands, whereas the current peak could be related to the thinnest ones. The theoretical results[16] suggest an opposite behavior, i.e., the current peak associated to the widest islands, and a soft bump for higher bias related to the thinnest islands. This prediction, however, is

for relatively low barriers and the relative intensity of the current peaks related to well regions of different thicknesses could be strongly dependent on the barrier heights.

A second important result shown in Fig. 2(a) is that an interisland transfer is already clear from the PLE experiment. Comparing the PL and PLE spectra, we find the largest emission related to the widest island. The largest PLE signal, on the other hand, is found to be associated to the thinnest well region. This implies that the thinnest growth islands probably cover the largest interface area,[13] which is also indicated by thermal activation measurements, discussed at the end of Sec. III C. An efficient interisland transfer would lead to PLE spectra that are not sensible to changes in the detection energy, as pointed out by Klann, Grahn, and Fujiwara.[13] We have also measured PLE with applied bias voltage. In this case, a background spectrum develops in the PLE curve which has a cutoff near 1.52 eV (below the threshold for absorption in the well), due to absorption in the *n*-type contact layers and consequent tunneling of electrons and holes to the quantum wells. We have also measured the temperature dependence of PL lines for low photoexcitation intensity under various bias values. We have observed a slight increase in PL intensity for the highest energy line, P_2, and a decrease of lowest energy line, P_1, with temperature at zero bias [Fig. 2(b)]. For higher temperatures the QW PL spectrum is superposed by the PL of contact layers and the analysis of temperature dependence is not possible. The integrated PL behavior with temperature can be qualitatively analyzed in the following terms. Radiative efficiency always decreases with temperature, so an increase of PL intensity should be associated with an increase of exciton population probably due to exciton transfer between islands. At higher temperatures the intensity of both lines decreases with temperature, which indicates that nonradiative processes dominate. By applying a bias voltage, we can change the populations in the islands and modify the temperature dependence of PL intensity. The temperature dependence will be further addressed in detail in the following sections of this work.

The PL intensity dependence with applied bias is as important as the temperature dependence. For low excitation intensity (0.5 W/cm^2) the PL intensity varies over an order of magnitude as a function of bias at low temperatures. Figure 3 shows typical PL spectra at $T=2$ K under reverse applied bias for excitation energy of 1.55 eV. In Fig. 3(a) the spectra are in the first resonant tunneling current peak bias range, while Fig. 3(b) shows PL spectra for bias at the onset of the second resonant tunneling peak. It is clear that two PL peaks are resolved for the whole bias range. An efficient intersubband transfer is already evident from Fig. 3(b), since electrons are injected resonantly into the E_2 quasibound state of the midwell, but a strong luminescence related to E_1-HH$_1$ transition is observed.

Figure 4 displays a careful mapping of the dependence of position, integrated intensity, and linewidth with bias for the PL peaks at low photoexcitation intensity. These features have been obtained by fitting the spectra by two Gaussian curves. V_n means absolute values for reverse (negative) bias polarization and will be used from now on in the following figures and discussions. The energy positions of both lines, Fig. 4(a), are bias independent, as expected for low excitation intensity and intrawell transitions. The absence of an

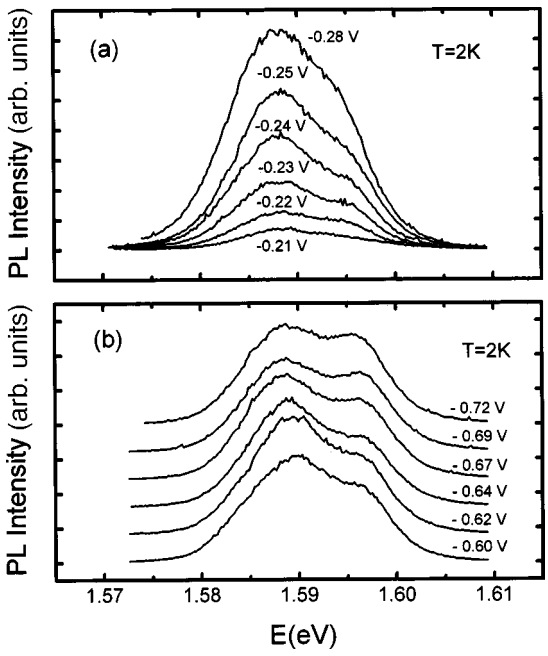

FIG. 3. PL spectra as a function of reverse bias for excitation energy of 1.55 eV under low photoexcitation intensity (0.5 W/m^2). (a) before first resonant current peak (b) before the second resonant current peak [see Fig. 1(b)].

appreciable Stark shift indicates a relatively large degree of localization, as suggested by the large PL linewidths. The possibility of crossed (interwell) transitions between prewell and midwell is disregarded, since the energy levels related to different layers of the structure would shift differently as a function of applied bias.[21] Furthermore, since the contact layers act as one of the barriers of each side (pre- and post-) well, transitions with energy higher than $E_g=1.52$ eV can only arise from the midwell with symmetrical and much higher AlAs barriers. The integrated PL intensity for both

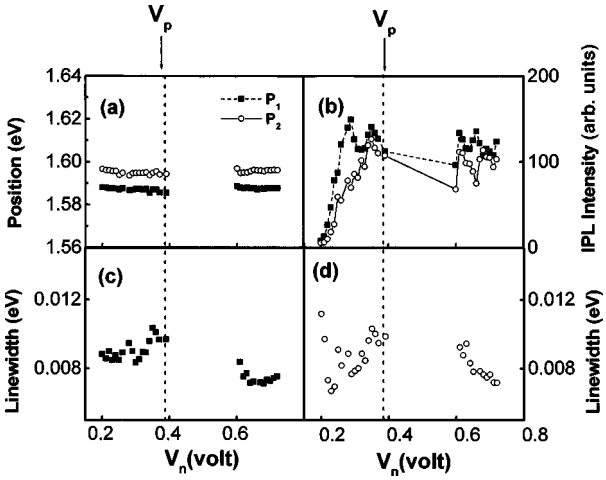

FIG. 4. (a) PL peak position for the two lines, P_1 and P_2 (lower and higher energies, respectively), as a function of bias; (b) integrated PL intensities; and (c), (d) PL linewidths (full width at half maximum) under low photoexcitation intensity (0.5 W/cm^2). V_p indicates the resonant tunneling peak position. V_n indicates that the measurements are for reverse bias polarization, the negative half axis in Fig. 1(b).

lines, Fig. 4(b), is very sensitive to bias voltage. At resonance, we have a strong increase of PL intensity as a function of bias voltage. In the presence of an applied bias voltage and under this excitation energy ($E_{ex}=1.55\,eV$), PL arises from recombination of tunneling electrons, whose density in the well builds up with increasing tunnel current, and holes which are photocreated in the contact region and are collected in the wells. There is a good correlation between the variation of integrated PL intensity and tunnel current with bias.[29] This correlation is expected in the low electron density regime, when hole recombination is dominated by nonradiative processes.[6,8] As the density of electrons in the mid-QW increases, radiative recombination of holes becomes dominant and the PL intensity first increases with bias and then saturates with further increase in electron density.[6,8] In our case, the density of electrons is distributed between different islands in the QW. For the lowest energy line we have some evidence of this saturation effect. As the bias voltage exceeds 0.28 V, the integrated PL intensity begins to saturate and becomes nearly independent of bias. Consistent with this picture is the slower increase, respective to bias, of the intensity of the second (higher energy, P_2) PL line. When the structure is biased above the resonant peak (onset of the second resonant tunneling peak) the total current increases while the luminescence remains relatively constant and high. This could be attributed to a decrease in electron and hole tunneling time with increasing bias, as well as a still high electron density, due to tunneling into the well followed by intersubband scattering.

We also observe a clear tendency of increasing linewidths in the resonance bias range for both lines, Figs. 4(c) and 4(d). This broadening arises from space charge buildup in the well with increasing tunnel current. The linewidth of the PL spectra in these structures will be controlled by the Fermi energy of the electrons in the QW and by the degree of hole localization or disorder in the system.[8,9]

B. High excitation intensity

Although self-contained, this scenario of growth island effects on optical and transport properties should be consistent with a high excitation intensity situation, which enhances the hole population in the midwell, while the electronic density still continues to be mostly determined by resonant tunneling injection.

A typical $I(V)$ characteristic under high photoexcitation intensity (60 W/cm^2) is shown in Fig. 5. We have observed a shift of resonant peak to lower voltages. Reductions of peak-to-valley ratio and bistability region are also observed. Such effects can be qualitatively understood by a higher photocreated hole density in the quantum-well region. This would partially compensate the well known screening of the external bias by the tunneling electrons,[30,31] leading to a reduction of the bistability region, as well as the voltage of the current peak. The reduction of the threshold voltage indicates an appreciable amount of electron heating in the emitter. This heating leads to an effective reduction of the necessary bias for resonant tunneling onset.

The PL spectra show an important qualitatively different behavior under high excitation intensity condition, compared to the low excitation intensity situation. On one hand, the total PL intensity increases, as expected from the increase in hole density in the midwell, which is consistent with the corresponding $I(V)$ characteristics as discussed above. Indeed we observe a linear increase of total PL intensity with excitation intensity for bias above the resonant tunneling onset, $V_n=0.25\,V$. On the other hand, however, there is an inversion in the relative intensities between the two luminescence peaks: under high excitation intensities, P_2 is much more intense than P_1. Figure 6(a) shows the dependence of integrated PL intensity with bias voltage. As under low excitation intensity, P_1 shows a saturation in the intensity before the tunneling resonances. However, the intensity of P_2 is now much higher than P_1, showing a very good correlation in respect to the tunneling current. It should be noticed that this correlation survives also for high bias voltages at the onset of the second resonance in tunneling current, $V_n > 0.6\,V$, and no saturation tendency is observed. This behavior reinforces a sequential tunneling picture:[28] electrons first tunnel resonantly into the well in the excited E_2 state and afterwards part of the electrons decay to the ground state, prior to tunneling out or recombining radiatively. Figure 6(b) shows the linewidth versus bias voltage for both lines. We have a still better correlation between linewidths and tunnel current for both peaks under high photoexcitation intensity. As discussed before, such an effect is expected since the linewidth is controlled by Fermi energy in the quantum well and by the degree of hole localization and disorder in the system.

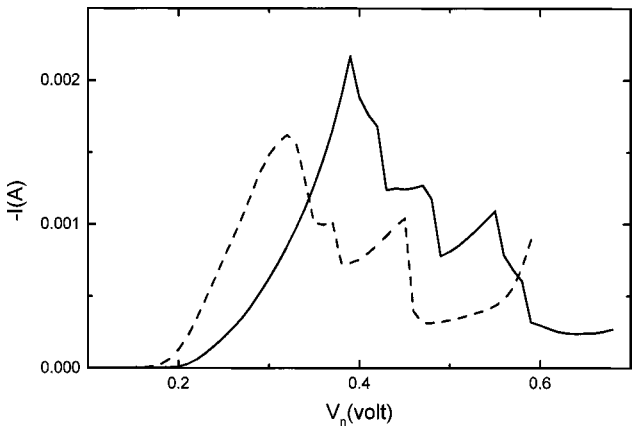

FIG. 5. $I(V)$ characteristics without illumination and with illumination (dashed line) under high photoexcitation intensity (60 W/cm^2).

C. Comparison between excitation intensity regimes

The results shown in Fig. 6 are actually consistent with those of Fig. 4(b), within the picture of two growth islands with one monolayer fluctuation between them, and are qualitatively explained in the framework of the model discussed by Skolnick *et al.*,[6] as well as by Andrews, Turberfield, and Miller.[31] The overall intensity of the luminescence is proportional to the hole density, whose increase is correlated to the increase in excitation intensity. Besides that, the PL intensity should present a linear dependence with electron density in the well, as long as one is in the nonradiative limit (hole escape by tunneling out of the well), otherwise, a saturation of the PL intensity is expected, irrespective of a further increase of electron density.[6] The electron density is mainly

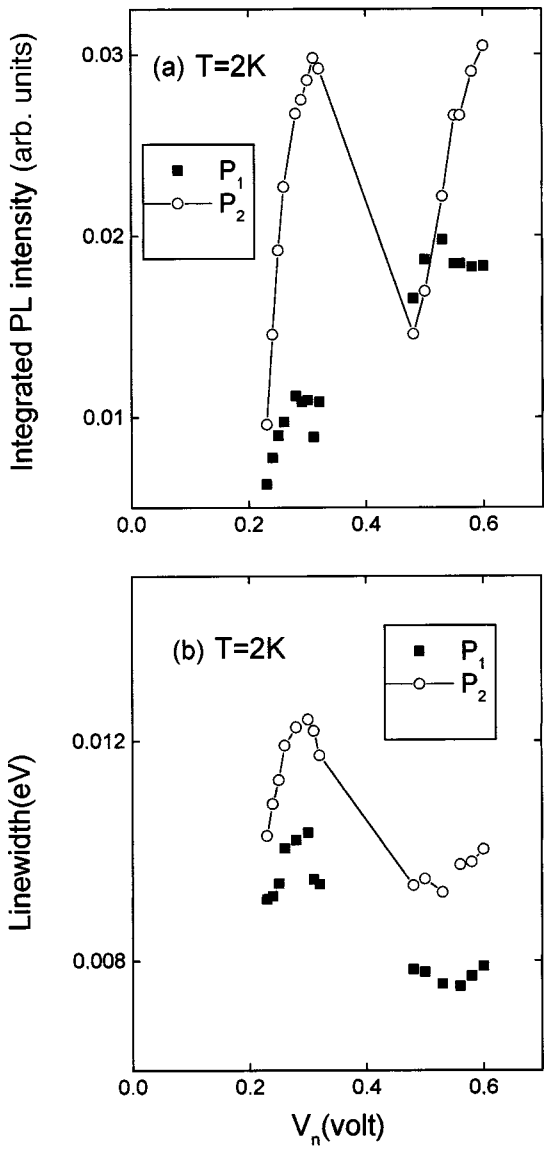

FIG. 6. (a) PL intensities and (b) linewidths as a function of bias under high photoexcitation intensity (60 W/cm^2). P_1 and P_2 are the lower and higher luminescence lines, respectively.

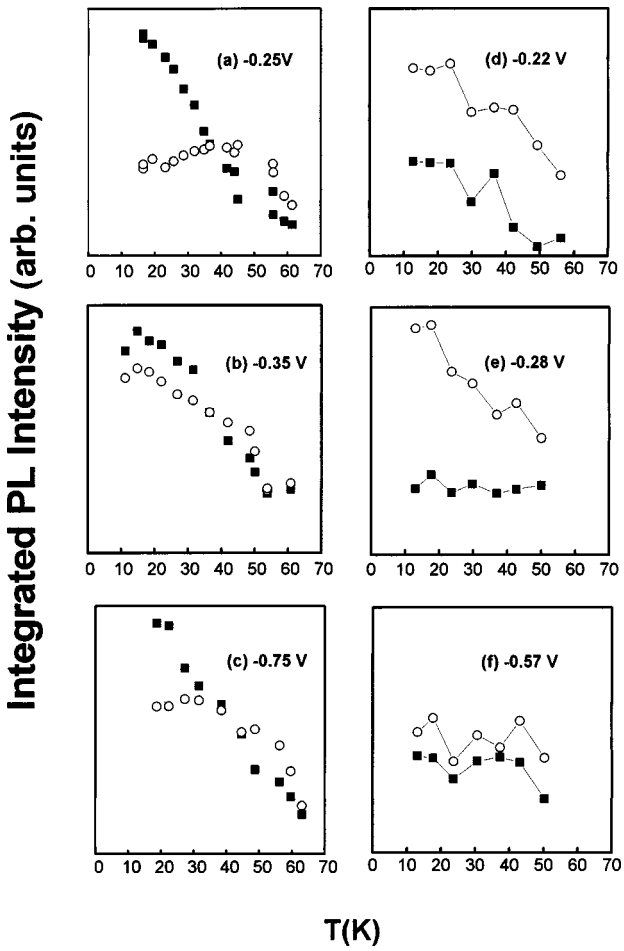

FIG. 7. Integrated PL intensity as a function of temperature for various bias voltages: Filled squares are for the low energy line (P_1) and open circles for the higher energy line (P_2). Low photoexcitation intensity (0.5 W/cm^2): (a) $V_n = 0.25$ V; (b) $V_n = 0.35$ V; and (c) $V_n = 0.75$ V. The same for high excitation intensity (60 W/cm^2): (d) $V_n = 0.22$ V; (e) $V_n = 0.28$ V; and (f) $V_n = 0.57$ V.

controlled by the bias voltage in the resonant tunneling range. We assume that in the presence of growth islands, the dominant transfer would be from thin islands (relative to P_2) to wide ones (relative to P_1). The backward transfer is inhibited by the potential step.[24] Therefore the saturation effect with electron density would predominantly occur for the lower energy luminescence line. Furthermore, under low excitation intensity, there is a stronger screening of the applied bias in the midwell, pinning the levels, leading to a lower injection of electrons by tunneling into the thin island levels (higher energy). Therefore, as already discussed, the intensity increase with bias of the P_2 line will be quite slow, besides being always less intense than P_1. For high excitation intensity, this screening effect is reduced, increasing the tunnel injection of electrons in the thin island levels. Furthermore, the electron injection by tunneling into the thin islands is also enhanced by the broadening of electron distribution in the emitter due to heating effects. Having in mind, however, a strong transfer rate from the thin island to the wide one, saturation of PL intensity would again occur for P_1.

An important investigating tool consists in tuning not only the radiative decay rate by changing the electron density in the well,[6] but also partially the nonradiative decay rate, by varying the temperature. Figure 7 shows the temperature dependence of integrated PL intensity for various biases before and after resonance. The left panels, Figs. 7(a)–7(c), are for low excitation intensity (0.5 W/cm^2). The right panels, Figs. 7(d)–7(f), are for high excitation intensity (60 W/cm^2). At the onset of resonant tunneling regime, Fig. 7(a), the density of electrons in the QW is still small and we have the same behavior as in the case of zero bias (low excitation intensity), not shown here. An additional effect here is seen above $T = 35$ K, where both lines show similar intensities, suggesting equally populated islands due to backward transfer mediated by inelastic scattering. Besides, raising the temperature, the PL intensity diminishes, due to enhancement of nonradiative decay. This is a general trend for all situations depicted in Fig. 7. Near the resonance peak for low excitation intensity, Fig. 7(b), we have a less significant temperature dependent transfer of carrier between islands, since both are almost equally populated with electrons due to resonant tunneling. After the resonance peak, Fig. 7(c), a low biaslike behavior, Fig. 7(a), is observed again. On one hand, electrons are more

effectively ejected from the QW and we can see that, as the density of electrons is lowered, the backward transfer of carriers between islands becomes again an important process as a function of temperature. On the other hand, the PL intensity is higher than at zero bias. Electrons at $V_n = 0.75$ V tunnel resonantly into the second quasibound state in the midwell and many of them decay to the first quasibound state before tunneling out or recombining at the measured PL related to the E_1-HH_1 line.

In the right panels of Fig. 7 we trace a parallel to similar bias conditions but for high excitation intensity. Here, the intensity of both PL lines also decreases with increasing temperature, which indicates that nonradiative processes become important. Furthermore, no significant backward transfer of carriers between islands is observed and no population equilibrium is obtained in the temperature range considered. This result is expected from the low temperature measurements, which, for bias range considered, show a P_2 line much more intense than P_1. The only exception is the very onset of the second resonance, $V_n = 0.57$ V, Fig. 7(f). Here electrons start to be injected resonantly again in the second quasibound state of the midwell followed by a fast relaxation to the lowest level of the wide island. However, due to the high bias, the escape rate for both islands is very high and the thin to wide island transfer mechanism in the midwell dominates. A further increase of bias will saturate the P_1 line.

The relative importance of backward transfer from wide to thin islands, due to thermal activation, can be clarified by means of Arrhenius plots of $I_2/I_1 \propto S_2/S_1^* \exp(-E_a/kT)$. S_2/S_1 reflects the ratio of the density of states of the corresponding quantum-well regions, and I_2/I_1 is the ratio between the integrated PL intensities of P_2 and P_1, respectively. Here E_a is the thermal activation energy and k, the Boltzmann constant. Figure 8 shows Arrhenius plots for different bias voltages and low excitation intensity. Near the onset of the first resonance we expect a very low electron density in the well. Therefore the backward transfer from the wide to the thin island should be characterized by an activation energy similar to the energy splitting of the PL lines ($\sim$8 meV) related to the monolayer fluctuation of different midwell regions.[32] Indeed, the activation energy for $V_n = 0.25$ V is $E_a = 8.6$ meV, Fig. 8(a). By increasing the bias voltage, the injected electron density in the midwell increases too. Considering the preferential transfer of electrons from thin to wide islands,[24] as well as a higher electron density in the wide islands, related to the precocious saturation of the P_1 line, the activation energy would diminish with increasing bias. Figure 8(b) shows the Arrhenius plot for $V_n = 0.35$ V, just before the resonant peak voltage. The slope of the line corresponds now to a lower activation energy ($E_a = 4$ meV), as expected from our interpretation. Indeed, ΔE_a gives an estimate of the electron density in the midwell. Multiplying ΔE_a by the constant 2D density of states, $\rho(E) = 4\pi m^*/h^2$, we obtain $n_e \sim 1.0 \times 10^{11}\,\mathrm{cm}^{-2}$, which is in reasonable agreement with values obtained for similar systems.[5,31] For bias values at the onset of the second resonance, Fig. 8(c), the same qualitative behavior is observed and the activation energy, $E_a = 7.3$ meV, is lower than at the onset of the first resonance. This reveals again the efficiency of the mechanism of tunneling through the second resonance followed by a fast decay to the ground level, enhancing the population of the last one. This result is consistent with the discussion in Sec. III A related to the saturation of P_1 for low excitation intensity at high bias, after the first resonance, Fig. 4(b).

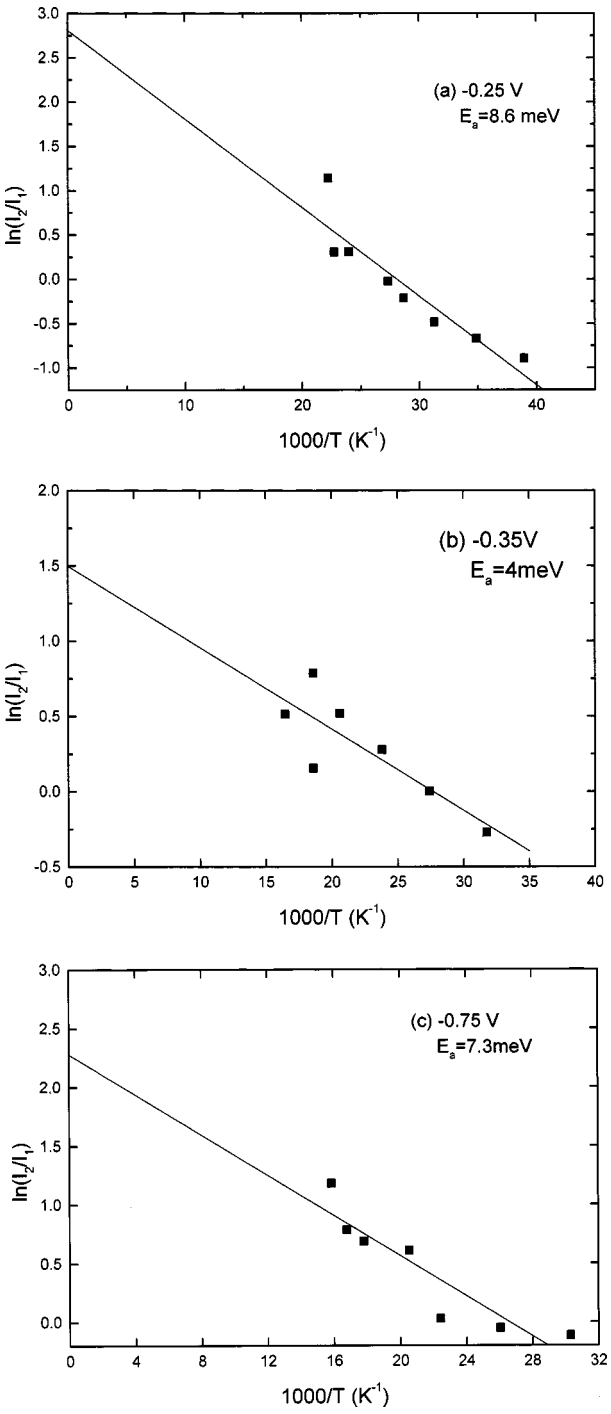

FIG. 8. Temperature dependence of the relative intensities of the PL lines, P_2 and P_1, under low photoexcitation intensity and different reverse bias voltages [see Figs. 7(a)–7(c)].

Additional and important information can be extracted from the extrapolation of the Arrhenius lines to infinite temperature, which gives the values for the corresponding prefactors $S_2/S_1 > 1$, independently from bias. This prefactor is proportional to the density of states ratio of both island regions and is consistent with the larger PLE signal for the

thinnest well region, Fig. 2(b), which implies that the thinnest growth islands cover the largest interface area,[13] as discussed in Sec. III A.

IV. CONCLUSIONS

In conclusion, we have identified growth island effects on resonant tunneling diodes by means of optical and transport spectroscopies. The present results are consistent with a picture of large growth islands together with strong microroughness at the interfaces. The large PL linewidth/Stokes-shift ratio also suggests that alloy disorder effects could be of the same order as those due to microroughness. The optical spectroscopy in the form of PL measurements reveals a double-peak structure in the spectra and all evidence supports the fact that each peak has an origin in different spatially separated regions of the central quantum well of the triple-well tunneling diode. The selective electron population of the island states is achieved by means of resonant tunneling. The hole population is mainly controlled by optical excitation intensity. Heating effects as well as screening reduction at high excitation intensities also equalizes the electron injection in the different islands. The presence of growth islands at the interfaces generates an interesting novelty regarding optical properties due to charge accumulation in resonant tunneling diodes, namely, a tunable internal structure of PL lines, where saturation effects may be observed for only one of them. Clear evidence for transfer of carriers from thin to wide islands is obtained in the resonant tunneling process under low photon excitation intensity. The backward transfer from wide to thin islands shows an activated behavior with temperature. The measurement of these activation energies as a function of bias gives a new way to estimate the electron density in the central well in a resonant tunneling situation. It is worth mentioning that clear evidence of sequential tunneling channels has been observed. This evidence appears in an interesting physical situation, where the optical properties are governed simultaneously by intersubband and interisland electron transfer. Finally, the present results lead to the quest of resolving island growth effects on the I-V characteristics in the suggested limit of high barriers and thin spacer layers. Further work, both theoretical and experimental, will be necessary in order to design resonant tunneling diodes, by varying barrier heights together with spacer layer widths, for which growth island features in the I-V characteristics may be differentiated from charge redistribution effects.

ACKNOWLEDGMENTS

The authors would like to acknowledge M. Maialle for helpful discussions and J. Nagle, B. Vinter, and Y. Guldner for the sample studied in this work. The financial support of Conselho Nacional de Desenvolvimento Científico e Tecnológico (CNPq), and Fundação de Amparo à Pesquisa do Estado de São Paulo (FAPESP) is also acknowledged.

*Author to whom correspondence should be addressed. Also at Departamento de Física, Universidade Federal de Santa Catarina, CP 476, Florianópolis-SC, 88040-900, Brazil. Electronic address: yara@power.ufscar.br

†Present address: Ecole Normale Supériere, 24, rue Lhomon, 75005 Paris, France.

‡Present address: Departamento de Física, Universidade Federal de São Carlos, CP 676, São Carlos-SP, 13565-905, Brazil.

[1] T. M. Fromhold, L. Eaves, F. W. Sheard, M. L. Leadbeater, T. J. Foster, and P. C. Main, Phys. Rev. Lett. **72**, 2608 (1994).

[2] A. K. Gein, P. C. Main, M. La Scala, Jr., L. Eaves, T. J. Foster, P. H. Baton, J. W. Sakai, F. W. Sheard, M. Henini, G. Hill, and M. A. Pate, Phys. Rev. Lett. **72**, 2061 (1994).

[3] T. J. Thornton, Rep. Prog. Phys. **58**, 311 (1995).

[4] P. S. Guimarães, Brian J. Keay, Jann Kaminski, S. J. Allen, Jr., P. F. Hopkins, A. C. Gossard, L. T. Florez, and J. P. Harbison, Phys. Rev. Lett. **70**, 3792 (1993).

[5] J. F. Young, B. M. Wood, G. C. Aers, R. L. S. Devine, H. C. Liu, D. Landheer, M. Buchanan, A. J. SpringThorpe, and P. Mandeville, Phys. Rev. Lett. **60**, 2085 (1988).

[6] M. S. Skolnick, P. E. Simmonds, D. G. Hayes, A. W. Higgs, G. W. Smith, A. D. Pitt, C. R. Whitehouse, H. J. Hutchinson, C. R. White, L. Eaves, M. Henini, and O. H. Hughes, Phys. Rev. B **42**, 3069 (1990).

[7] M. S. Skolnick, D. G. Hayes, P. E. Simmonds, A. W. Higgs, G. W. Smith, H. J. Huchinson, C. R. Whitehouse, L. Eaves, M. Henini, O. H. Hughes, M. L. Leadbearer, and D. P. Halliday, Phys. Rev. B **41**, 10 754 (1990).

[8] T. H. Wang, X. B. Mei, C. Jiang, Y. Uang, J. M. Zhou, and G. Z. Yang, Appl. Phys. Lett. **62**, 1149 (1993).

[9] D. Bertram, H. T. Grahn, C. Van Hoof, J. Genoe, G. Borghs, W. Rühle, and K. Von Klitzing, Phys. Rev. B **50**, 17 309 (1994).

[10] H. Buhmann, L. Mansouri, J. Wang, P. H. Beton, N. Mori, L. Eaves, M. Henini, and M. Potemski, Phys. Rev. B **51**, 7969 (1995).

[11] Z. C. Yan, E. Goovaerts, C. VanHoof, A. Bouwen, and G. Borghs, Phys. Rev. B **52**, 5907 (1995).

[12] M. J. S. Brasil, R. E. Nahory, M. C. Tamargo, and S. A. Schwarz, Appl. Phys. Lett. **63**, 2688 (1993).

[13] R. Klann, T. Grahn, and F. Fujiwara, Phys. Rev. B **51**, 10 232 (1995).

[14] P. Johansson, Phys. Rev. B **48**, 8938 (1993), and references therein.

[15] W. T. Dietze and B. Darling, Phys. Rev. B **53**, 3925 (1996).

[16] Shui-Jinn Wang, Jia-Chuan Lin, Wan-Rone Liou, Mei-Ling Yeh, Ying-Che Luo, and Ching-Yuan Cheng, Jpn. J. Appl. Phys., Part 1 **35**, 3582 (1996).

[17] H. Sakaki, H. Yashimura, M. Tsuchiya, and T. Matsusue, in *Resonant Tunneling in Semiconductors*, edited by L. L. Chang, E. E. Mendez, and C. Tejedor (Plenum, New York, 1991), p. 307.

[18] M. K. Jackson, M. B. Johnson, D. H. Chow, T. C. McGill, and C. W. Nieh, Appl. Phys. Lett. **54**, 522 (1989).

[19] P. Gueret and C. Rossel, in *Resonant Tunneling in Semiconductors*, edited by L. L. Chang, E. E. Mendez, and C. Tejedor (Plenum, New York, 1991), p. 71.

[20] L. Burgnies, O. Vanbesien, V. Sadaune, D. Lippens, J. Nagle, and B. Vinter, J. Appl. Phys. **75**, 4527 (1994).

[21] P. H. Rivera and P. A. Schulz, Appl. Phys. Lett. **67**, 2675 (1995).

[22] M. V. Marquezini, M. J. S. P. Brasil, J. A. Brum, P. Poole, S. Charboneau, and M. C. Tamargo, Phys. Rev. B **53**, 16 524 (1996).

[23] M. V. Marquezini, M. J. S. P. Brasil, M. A. Cotta, J. A. Brum, and A. A. Bernussi, Phys. Rev. B **53**, R16 156 (1996).
[24] B. Deveaud, T. C. Damen, J. Shah, and C. W. Tu, Appl. Phys. Lett. **51**, 828 (1987).
[25] M. Tsuchiya, T. Matsutue, and H. Sakaki, Phys. Rev. Lett. **59**, 2356 (1987).
[26] M. Wilkinson, F. Yang, E. J. Austin, and K. P. O'Donnell, J. Phys.: Condens. Matter **4**, 8863 (1992).
[27] R. Zimmermann, E. Runge, and F. Grosse, in *Proceedings of the 23rd International Conference of Physics of Semiconductors*, edited by M. Scheffler and R. Zimmermann (World Scientific, Singapore, 1996), p. 1935.
[28] T. K. Woodward, D. S. Chemla, I. Bar-Joseph, H. U. Baranger, D. L. Sivco, and A. Y. Cho, Phys. Rev. B **44**, 1353 (1991).
[29] Y. Galvão-Gobato, A. L. C. Triques, P. H. Rivera, P. A. Schulz, Y. Guldner, and B. Vinter, J. Appl. Phys. **82**, 810 (1997).
[30] F. W. Sheard and G. A. Toombs, Appl. Phys. Lett. **52**, 1228 (1988).
[31] S. R. Andrews, A. J. Turberfield, and B. A. Miller, Phys. Rev. B **47**, 15 705 (1993).
[32] U. Jahn, S. H. Kwok, M. Ramsteiner, R. Hey, and H. T. Grahn, Phys. Rev. B **54**, 2733 (1996).